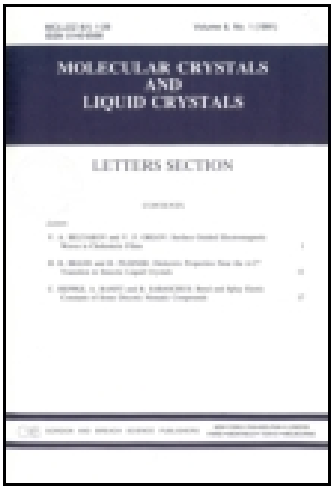

Molecular Crystals and Liquid Crystals
Publication details, including instructions for authors and subscription information:
http://www.tandfonline.com/loi/gmcl20

Dynamic Holography Recording on E204Q Bacteriorhodopsin Gelatin Films in Red-Light Range at Different Humidity Values

Elena Korchemskaya [a b], Dmitrij Stepanchikov [c], Nikolai Burykin [a], Tatyana Dyukova [d], Sergei Balashov [e] & Alla Savchuk [a]

[a] Institute of Applied Optics, National Academy of Sciences of Ukraine, Kiev, Ukraine

[b] Institute of Physics, National Academy of Sciences of Ukraine, Kiev, Ukraine

[c] Zhytomir State University, Ukraine

[d] Institute of Theoretical and Experimental Biophysics, Russian Academy of Sciences, Pushchino, Russia

[e] University of California, Irvine, USA

Published online: 28 Mar 2014.

To cite this article: Elena Korchemskaya, Dmitrij Stepanchikov, Nikolai Burykin, Tatyana Dyukova, Sergei Balashov & Alla Savchuk (2014) Dynamic Holography Recording on E204Q Bacteriorhodopsin Gelatin Films in Red-Light Range at Different Humidity Values, Molecular Crystals and Liquid Crystals, 589:1, 232-241, DOI: 10.1080/15421406.2013.872853

To link to this article: http://dx.doi.org/10.1080/15421406.2013.872853

Mol. Cryst. Liq. Cryst., Vol. 589: pp. 232–241, 2014

ISSN: 1542-1406 print/1563-5287 online
DOI: 10.1080/15421406.2013.872853

Dynamic Holography Recording on E204Q Bacteriorhodopsin Gelatin Films in Red-Light Range at Different Humidity Values

ELENA KORCHEMSKAYA,[1,2,*] DMITRIJ STEPANCHIKOV,[3] NIKOLAI BURYKIN,[1] TATYANA DYUKOVA,[4] SERGEI BALASHOV,[5] AND ALLA SAVCHUK[1]

[1]Institute of Applied Optics, National Academy of Sciences of Ukraine, Kiev, Ukraine
[2]Institute of Physics, National Academy of Sciences of Ukraine, Kiev, Ukraine
[3]Zhytomir State University, Ukraine
[4]Institute of Theoretical and Experimental Biophysics, Russian Academy of Sciences, Pushchino, Russia
[5]University of California, Irvine, USA

The effect of humidity on the holographic grating diffraction efficiency and transmittance kinetics in the E204Q BR gelatin film is investigated. We found a correlation between the accumulation of the red-light absorbing O intermediate in the later part of the E204Q BR photocycle and sharpness (decay to the steady-state) of the holographic recording kinetics. As shown, at humidity exceeding 95% the ratio between the peak and steady-state of the diffraction efficiency for the weak probe beam (670 nm) can reach 8.7 in the E204Q BR film, which is sufficient for realization of an efficient novelty filter.

Keywords E204Q bacteriorhodopsin mutant; gelatin films; dynamic holography; relative air humidity; novelty filter

Introduction

Purple membrane containing bacteriorhodopsin (BR), a light-driven proton pump and light-transducing photoreceptor protein from the microorganism *Halobacterium salinarum* [1, 2] possesses unique photochemical and photophysical properties in terms of workability in polymer films or blocks for device applications [3]. For dynamic holography recording, BR polymer films are very promising because they have a high spatial resolution, are reversible and stable enough to permit millions of read–write cycles without degradation of the film quality [4–7]. Both the BR wild type (the form which is found in nature) and BR genetic mutants are a subject of active interest for dynamic holography [7–10]. The genetic engineering of BR became a powerful tool for the design of novel photochromic materials enabling to construct mutants with desired properties and performance characteristics.

*Address correspondence to Dr. Elena Korchemskaya, Institute of Physics, National Academy of Sciences, 46 Prospect Nauki, Kiev, 03028 Ukraine; Tel.: +380-44-286 5735, 525 0813. Fax: +380-44-525 1589. E-mail: elkorch@iop.kiev.ua

Upon illumination, BR transports protons across the membrane and undergoes reversible light-induced transitions through a set of photocycle intermediates: $B_{570} \rightarrow K_{610} \rightarrow L_{540} \rightarrow M_{412} \rightarrow N_{550} \rightarrow O_{640} \rightarrow B_{570}$. The letters denote the ground state ("B") and intermediate states ("K" to "O", respectively), and the subscripts refer to the wavelengths in nm of their absorption maxima. A large photochromic shift occurs during the light-adapted-BR photocycle. With dynamic holographic grating recording, the interference of two coherent laser beams modulates the light intensity at the BR film plane. This leads to the spatial modulation of the accumulated BR photoproducts. Usually, the B- and M-states are the most populated in the dry polymer films with the wild type (WT) BR and its genetic mutants.

Important for optical and holographic applications of BR polymer films is to find the conditions for a considerable population of the red-light absorbing states, because a red-light range is very attractive for practical applications due to the suitability of compact low-power semiconductor lasers. However, pulse high-power lasers are required to form the photocycle intermediate K [11] and two-photon-absorption photoproduct F_{620} [12] in the WT BR polymer films in the amounts sufficient for applications. Also a small amount of the photocycle intermediate O in the WT BR film was detected under the cw gas laser excitation [13].

It was shown that the yield of the O intermediate is much higher in the suspension of the genetic mutant E204Q BR than in the WT BR due to a decreased rate of O to BR transition [14, 15]. The replacement of E204 with non-ionazable glutamine in E204Q BR, the site-specific mutation in BR at the extracellular side, disables the proton release cluster. Substitution of E204 alters the proton release behaviour of BR [16].

As known, the relative air humidity strongly affects the photocycle of BR in purple membrane fragments [17, 18]; it also exerts the dramatic influence on the photoconversions of WT BR in a thin gelatin film [19]. Recently, we have found that in the E204Q BR thin gelatin film at high water content a considerable amount of BR molecules under the action of a cw gas He-Ne laser ($\lambda = 633$ nm) undergoes the photocycle involving red-light absorbing O intermediate [7]. In the present paper, the holographic grating diffraction efficiency, transmittance and thermal-decay kinetics in the E204Q BR gelatin film at humidity values from 60 to 98% are investigated for a red-light range. A cw gas He-Ne laser ($\lambda = 633$ nm) is used for the transmission thin grating recording. The transmittance and diffraction efficiency kinetics are measured on wavelengths of 633 and 670 nm. A measurement of the transmittance on a wavelength of 670 nm allows for detecting just the O-state accumulation (without a contribution from an accumulation of other photocycle intermediates) [20]. It enabled us to find a correlation between the O-state accumulation and the grating recording kinetics on 633 nm at different humidity values. The diffraction efficiency behaviour is a main prerequisite for a novelty filter with the use of a BR film [21].

Materials and Methods

E204Q BR film. An aqueous suspension of the genetic mutant E204Q BR was mixed at 35–40°C with an aqueous 8% gelatin solution and the pH of the mixture brought to 7.3. The mixture was then applied (by flowing) on a 1 mm-thick optical glass support to form a thin layer. The thickness of the dried film at ambient humidity is approximately 40–50 μm. The maximum absorbance of the light-adapted E204Q BR films at 560 nm was about 2.2–2.7. The film preparation protocol has been previously described in detail [22].

Experimental technique. To study the effect of humidity on the holographic recording and transmittance kinetics in E204Q BR gelatin film, an optical glass support with E204Q

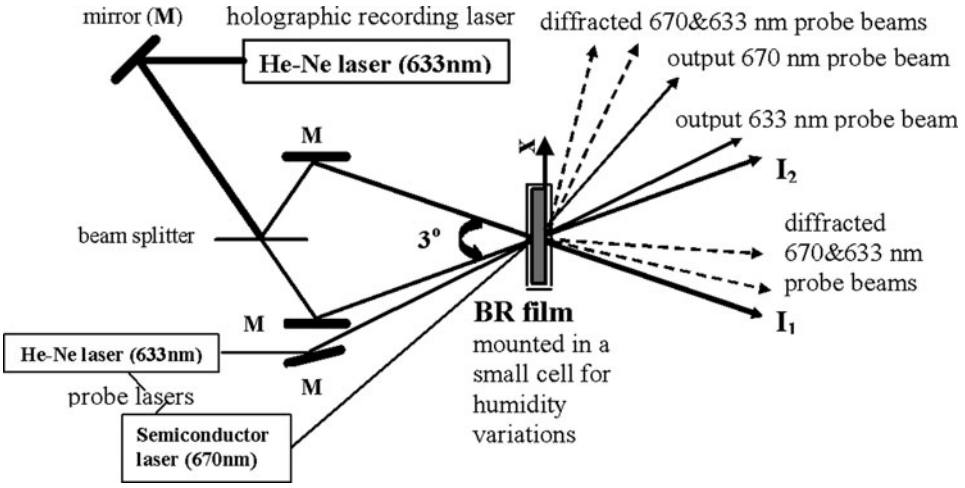

Figure 1. Experimental setup for transmission thin grating recording and detecting light-induced absorption changes. A holographic grating is recorded at 633 nm and probed at 633 nm and 670 nm. The light-induced absorption changes are also probed both at 633 nm and 670 nm. E204Q BR film is mounted in a miniature cell to modify and control humidity.

BR film was fixed on the inside wall of a miniature hermetic cell [19]. Mounting the cell (with a BR film) in the holographic set-up allowed us to perform holographic measurements on the film at a fixed humidity from 60 to 98% over long periods of time.

A cw He-Ne laser with $\lambda = 633$ nm was used for holography grating recording. For probing the time course of the grating recording, the He-Ne laser with $\lambda = 633$ nm and semiconductor laser with $\lambda = 670$ nm were used. A beam from the recording He-Ne laser is split into two beams I_1 and I_2 of equal intensity $I_{1,2} = 200$ mW/cm^2. These two plane waves were recombined with an angle of 3° between them to form an interference pattern at the BR film plane X (Fig. 1). Under these conditions, thin transmission grating with spacing of approximately 40 μm is recorded in the BR film.

For a maximum diffraction efficiency, a probe beam with a wavelength of 633 nm, but not coherent with the recording beams having an intensity of 8 mW/cm^2 was directed on the BR film at nearly Bragg angle. Also the probe semiconductor laser beam with a wavelength of 670 nm and intensity of 3 mW/cm^2 was directed on the BR film. The intensities of the probe He-Ne laser and semiconductor laser beams were sufficiently weak and exerted a negligible erasing effect on the grating recorded in the film. The kinetics of the symmetric first-order diffracted probe beams and output probe beams were measured by the digital storage oscilloscopes TDS2014 (Tektronix).

The diffraction efficiency of the grating η is defined as the intensity in the diffracted probe beam divided by the intensity in the input probe beam. The diffraction efficiencies of the symmetric first-order diffracted probe beams are equal at 60–98% humidity range. These are obtained under Raman-Nath thin grating conditions only [23] and hence the diffraction efficiency at the recombined angle of 3° does not depend on the conceivable variation in the gelatin film thickness at different humidities. Thus, the changes in the diffraction efficiencies kinetics at different humidity values will be the representative of photoconversions in the gelatin- entrapped purple membrane fragments.

The transmittance of BR film is detected as the intensity in the output probe beam divided by the intensity in the input probe beam. The transmittance kinetics was measured

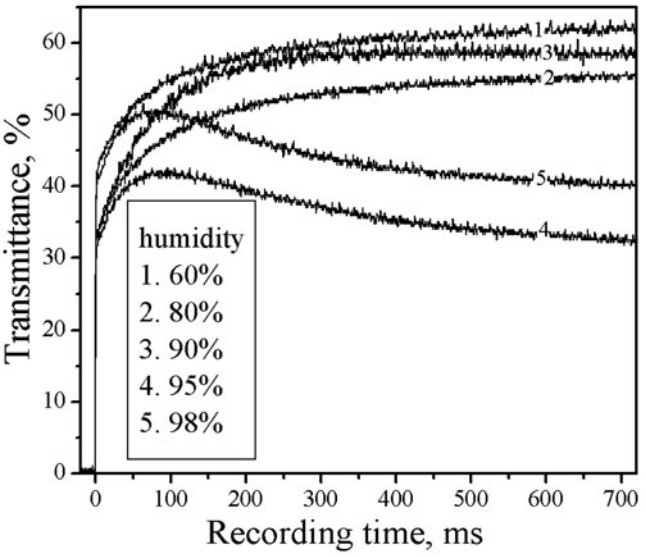

Figure 2. Transmittance kinetics at 633 nm during the recording process with a He-Ne laser at 633 nm at different humidity values.

on the wavelengths of 633 and 670 nm during and after the recording process made with a He-Ne laser at 633 nm (Fig. 1).

Results and Discussion

We have examined the probe beam transmittance at 633 and 670 nm during and after holographic grating recording at the wavelengths of 633 nm at different humidity values. Data sets at relative humidity values of 60%, 80%, 90%, 95% and 98% were recorded. To start a data set, the gelatin film made with E204Q BR was kept in the dark for 24 hours at 60% humidity inside the cell. Then the film was light-adapted by the He-Ne laser beam I_2 (Fig. 1) for three hours. The holographic grating recording was carried out for 5 min after turning off the light-adaptation beam. To measure the transmittance and grating recording kinetics at 80% relative humidity, the BR film was kept in the dark for 24 hours at this humidity inside the cell. Then again the film was exposed to 3-hours of uniform red light and next, the grating recording and transmittance kinetics were measured within 5 min after of turning off the light- adaptation beam. The similar procedure was used for all other humidity values.

The transmittance kinetics for the probe beam with 633 nm during recording at different humidity values is shown in Fig. 2. It is seen that at humidity values of 60–90% a transmittance increases monotonically to a steady-state which is typical for the photobleaching process in BR films.

A two-state photochemical cycle model, B↔M seems sufficient for a quantitative model of this kinetics [5, 10]. The transmittance kinetics at humidity values of 95 and 98% increase to a peak value, and then decrease toward a steady-state. Such behavior cannot be explained only by B↔M transitions. This result points to the formation of the red-light absorbing intermediate in the later part of a photocycle causing a decrease in a transmittance of the 633 nm probe beam. Since it is known that the accumulation of the O intermediate

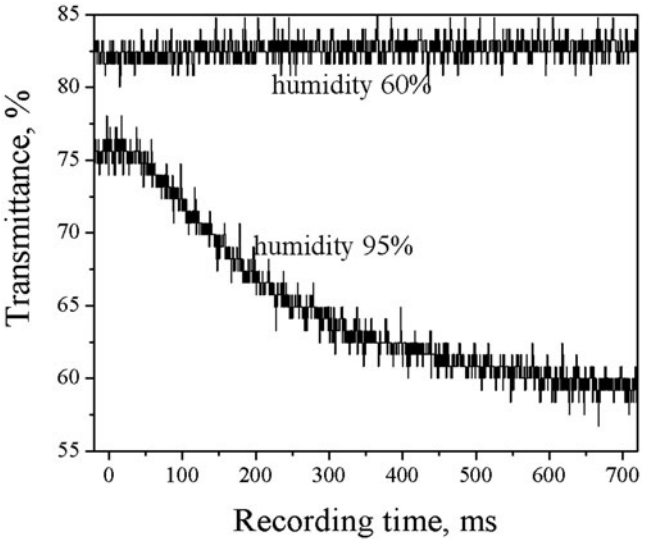

Figure 3. Transmittance kinetics at 670 nm during the recording process with a He-Ne laser at humidity values of 60% and 95%.

in the E204Q BR suspension is much higher than in the WT BR [14, 15], we suggest that O intermediate might be formed in the E204Q BR film at high humidity values. To check the assumption, we measured the transmittance kinetics for a 670 nm probe beam during the recording with He-Ne laser (633 nm) at humidity values of 60 and 95% (Fig. 3).

It is known that the transmittance on 670 nm is directly represents the O intermediate accumulation [20]. A transmittance on 670 nm at 95% humidity markedly decreases over nearly 50 ms from the recording time, whereas a transmittance at 60% humidity is practically constant during recording. This can indicate that the considerable population of O intermediate arises in the E204Q BR film at humidity values of 95%. The transmittance kinetics on 670 nm at 95% humidity after the recording process with a He-Ne laser at 633 nm demonstrates a slow increase, while the transmittance kinetics at 60% humidity is unchanged after the recording process as well (Fig. 4).

The transmittance kinetics on 633 nm after the recording process with a He-Ne laser at different humidity values is shown in Fig. 5.

A transmittance after recording decreases at any humidity value. The regressive analysis of the optical density decay on 633 nm after a He-Ne laser recording at humidity values of 60, 80 and 98% is carried out by the least square method (Fig. 6). A transmittance T and optical density D are interconnected:

$$D = -\lg(T). \tag{1}$$

It is seen that optical density decay is well described by a single exponential at humidity values of 60 and 80% (Fig. 6, curves 1 and 2):

$$D = D_0 - (D_0 - D_{st}) \exp(-k_{M\to B} t), \tag{2}$$

where D_{st}, D_0 and D are optical densities of a sample at a steady-state under recording, within a long time after recording and at given time of recording, correspondingly. Usually,

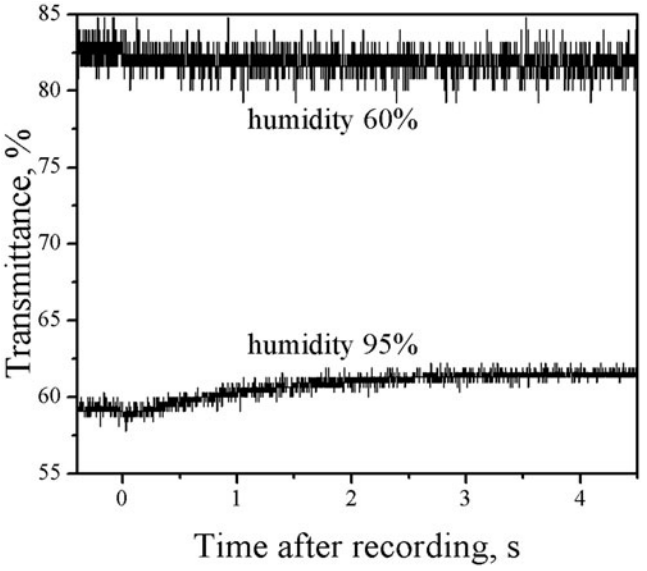

Figure 4. Transmittance kinetics at 670 nm after the recording process with a He-Ne laser at humidity values of 60% and 95%.

a speed of the thermal relaxation M→B for BR films, $k_{M\to B} = 0.95\ c^{-1}$ [5]. Hence, the relaxation M→B takes place in the E204Q BR film at humidity values of 60 and 80% without substantial accumulation of the O intermediate.

At high humidity (Fig. 6, curve 3), a decay is appreciably accelerated and proceeds with several exponential components. The moderate optical density changes do not allow

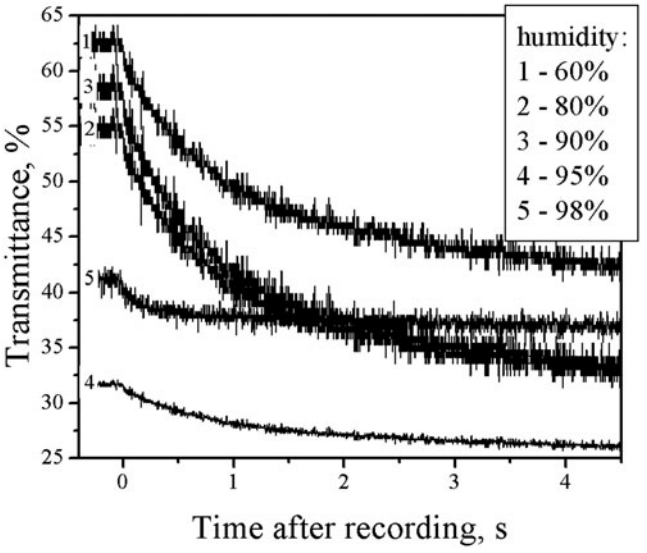

Figure 5. Transmittance kinetics at 633 nm after the recording process with a He-Ne laser at different humidity values.

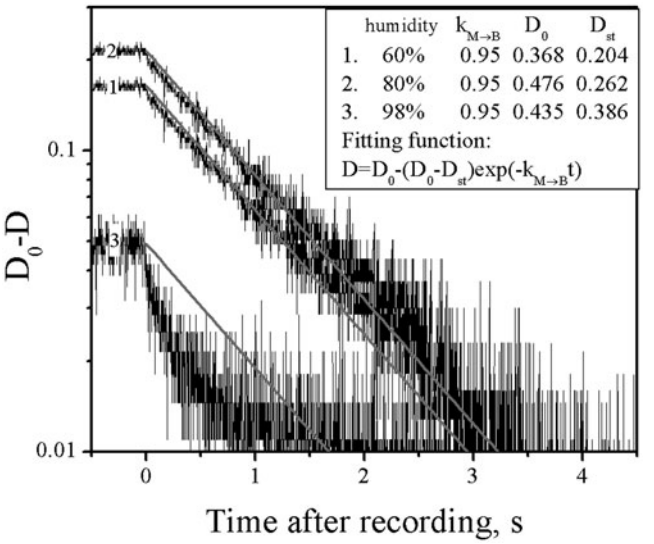

Figure 6. Optical density decay kinetics at 633 nm after the recording process with a He-Ne laser at humidity values of 60, 80 and 98% and their regressive analysis as a single exponential by the least square method (grey lines).

us to determine the parameters of these components precisely. It follows that optical density decay in the E204Q BR film at humidity value of 98% cannot be described just by M→B relaxation scheme.

The holographic grating diffraction efficiency kinetics of probe beam with 633 nm wavelength during the recording process with a He-Ne laser at different humidity values is presented in Fig. 7.

The grating recording kinetics consists of two stages: an initial increase to a maximum value (a peak) followed by a decrease to a steady-state due to low-saturation absorption of the E204Q BR film [7] at all humidity values. A maximum value of the diffraction efficiency is reached at humidity value of 90%. We have shown that the initial peak sharpness (decay to the steady-state) increases with increasing humidity values. It correlates with a decline in a probe beam transmittance on 633 nm (Fig. 2) and 670 nm (Fig. 3) at high humidity values. As is seen from Fig. 3, during the initial peak of diffraction efficiency (see Fig. 7 for details), a population of O intermediate is yet insignificant but it accumulates with time and causes the decrease in transmittance of the red probe beam. Upon probing the E204Q BR film by the 633 nm laser beam at high humidity, a steady-state in diffraction efficiency kinetics shows the extra-fall due to the formation of O intermediate in the later part of the photocycle.

A significant increase in the ratio between the peak and steady-state values of diffraction efficiency is reached for the 670 nm probe beam (Fig. 8). For probing by a low-power semiconductor laser with a wavelength of 670 nm, the ratio between the peak and steady-state values is 8.7, whereas it is 4.2 for probing by the He-Ne laser at 633 nm. It adds considerable support for the contribution made by O-state accumulation in the later part of the photocycle to the sharpness of the holographic grating recording kinetics in the E204Q BR gelatin film. This feature is extremely useful for the development of a novelty filter which is based on the time-dependent nonlinear diffraction efficiency of real-time

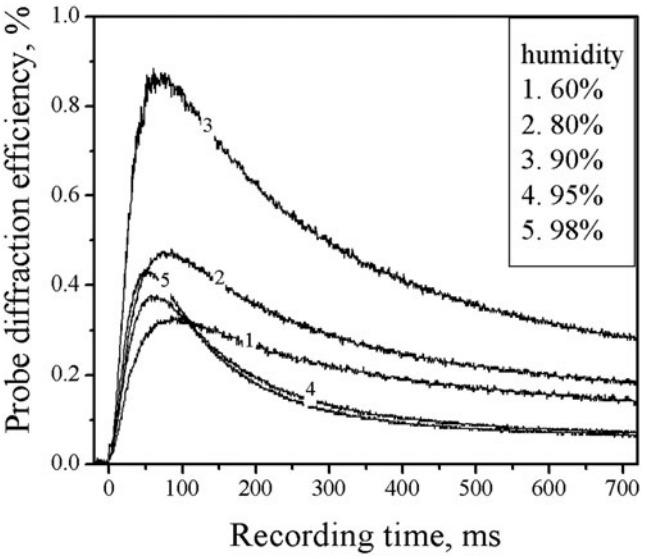

Figure 7. Diffraction efficiency kinetics of the probe beam, $\lambda = 633$ nm, during the recording process with a He-Ne laser at different humidity values.

holograms recorded in the BR film [21]. Earlier, the high-power Ar^+ laser ($\lambda = 514.5$ nm) was used as the signal beam for suppressing the diffraction of the beam at the position of the stationary part of the pattern. To obtain the ratio between the peak and steady-state values of diffraction efficiency as high as of 8, the intensity of the signal beam from the Ar^+ laser should be more than 5 W/cm^2.

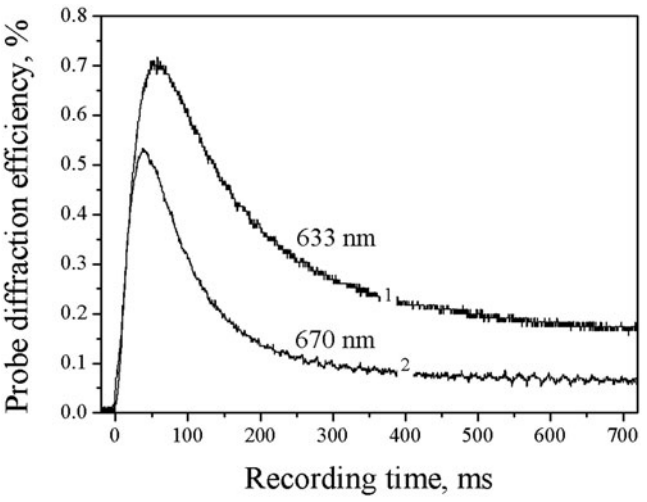

Figure 8. Diffraction efficiency kinetics of probe beams, wavelengths 633 nm (curve 1) and 670 nm (curve 2) during the recording process with a He-Ne laser at 95% humidity.

We found that the E204Q BR gelatin film mounted in the cell with the humidity value higher than 95% allows one to apply as the signal beam the semiconductor laser beam with a wavelength of 670 nm and intensity of only 3 mW/cm^2.

In conclusion, we have observed the O-state accumulation (without a contribution from other intermediates) in the E204Q BR gelatin film depending on humidity values. It allowed us to find the direct correlation between the red-light absorbing 'O' accumulation in the later part of the photocycle in the E204Q BR film and sharpness (decay to the steady-state from a peak value) of the holographic grating recording kinetics at different humidity values. Under the recording of a He-Ne laser, a population of O intermediate is yet insignificant during the initial peak of the diffraction efficiency kinetics, but the time of O accumulation matches the decay to the steady-state. A considerable amount of the O intermediate causes the decrease in transmittance of the red probe beams. We demonstrate that for the weak semiconductor laser probe beam, 670 nm (absorbed by just O intermediate), the ratio between the peak and steady-state values of diffraction efficiency can reach 8.7 in the E204Q BR at the humidity exceeding 95%, whereas it is 4.2 for probing by the He-Ne laser, 633 nm. Thus, the extra-suppression of the diffraction efficiency at the position of the stationary part of a signal can be obtained from the decrease in transmittance of the 670 nm probe beam solely due to the formation of the O intermediate. It opens a way for the realization of the novelty filter based on the time-dependent nonlinear diffraction efficiency of dynamic holograms in the E204Q BR gelatin film by using compact low-power red lasers.

Acknowledgments

The research described in this publication was made possible in part by Award No. UB2-2427-KV-02 of the U.S. Civilian Research & Development Foundation for the Independent States of the Former Soviet Union (CRDF) to E.K., D.S., N.B., and S.B.

References

[1] Oesterhelt, D., & Stoeckenius, W. (1973). *Proc. Natl. Acad. Sci. U.S.A.*, *70*, 2853.
[2] Balashov, S. P. & Lanyi, J. K. (2006). Bacteriorhodopsin. In *Microbial Bionanotechnology*, Rehm, B. (Ed.), Horizon Press, London, 339–365.
[3] Vsevolodov, N. N. (1998). *Biomolecular Electronics. An Introduction via Photosensitive Proteins*, Birkhauser, Boston.
[4] Zhang, Y.-H., Song, Q.W., Tseronis, C. & Birge, R.R. (1995). *Optics Letters*, *20*, 2429.
[5] Downie, J. D. & Timucin, D. A. (1998). *Applied Optics*, *37*, 2102.
[6] Korchemskaya, E., Stepanchikov, D., & Burykin, N. (2001). In: *Bioelectronic Applications of Photochromic Pigments*, Der, A. & Keszthelyi, L. (Eds.), IOS Press, Amsterdam, 74–89.
[7] Burykin, N., Stepanchikov, D., Dyukova, T., Savchuk, A., Balashov, S., & Korchemskaya, E. (2011). *Mol. Cryst. Liq. Cryst.*, *535*, 140.
[8] Hampp, N., Popp, A., Brauchle, C., & Oesterhelt, D. (1992). *J. Phys. Chem.*, *96*, 4679.
[9] Hillebrecht, J. R., Wise, K. J., Koscielecki, J. F., & Birge, R. R. (2004). *Methods Enzymol.*, *388*, 333.
[10] Stepanchikov, D., Burykin, N., Dyukova, T., Ebrey, T., Balashov, S., & Korchemskaya, E. (2006). *Functional Materials*, *13*, 669.
[11] Fábián, L., Heiner, Z., Mero, M., Kiss, M., Wolff, E. K., Ormos, P., Osvay, K., & Dér, A. (2011). *Optics Express*, *19*, 18861.
[12] Yao, B., Lei, M., Ren, L., Menke, N., Wang, Y., Fischer, T., & Hampp, N. (2005). *Opt. Lett.*, *30*, 3060.
[13] Popp, A., Wolperdinger, M., Hampp, N., Bruchle, C., & Oesterhelt, D. (1993). *Biophys. J.*, *65*, 1449.

[14] Brown, L., Sasaki, J., Kandori, H., Maeda, A., Needleman, R., & Lanyi, J. (1995). *J. Biol. Chem.*, *270*, 27122.
[15] Hillebrecht, J. R., Koscielecki, J. F., Wise, K. J., Marcy, D. L., Tetley, W., Rangarajan, R., Sullivan, J., Brideau, M., Krebs, M. P., Stuart, J. A., & Birge, R. R. (2005). *Nanobiotechnology*, *1*, 141.
[16] Misra, S., Govindjee, R., Ebrey, T. G., Chen N., Ma, J.-X., & Crouch, R. K. (1997). *Biochemistry*, *36*, 4875.
[17] Korenstein, R., & Hess, B. (1977). *Nature*, *270*, 184.
[18] Murata, K., Fujii, Y., Enomoto, N., Hata, M., Hoshino, T., & Tsuda, M. (2000). *Biophys. J.*, *79*, 982.
[19] Korchemskaya, E., Burykin, N., Bugaychuk, S., Maksymova, O., Ebrey, T., & Balashov, S. (2007). *Photochem. Photobiol.*, *83*, 403.
[20] Gillespie, N. B., Wise, K. J., Ren, L., Stuart, J. A., Marcy, D. L., Hillebrecht, J., Li, Q., Ramos, L., Jordan, K., Fyvie, S., & Birge, R. R. (2002). *J. Phys. Chem. B*, *106*(51), 13352.
[21] Okamoto, T., Yamaguchi, I., Boothroyd, S. A., & Chrostowski, J. (1997). *Applied Optics*, *36*, 508.
[22] Dyukova T., & Lukashev, E. (1996). *Thin Solid Films*, *283*, 1.
[23] Eichler, H. I., Gunter, P., & Pohl D. W. (1986). *Laser-induced dynamic gratings*. Springer-Verlag, Berlin.